Data dimensionality reduction for an optimal switching mode classification applied to a step-down power converter

LUIS-ALFONSO FERNANDEZ-SERANTES*, *Department of Industrial Engineering, University of A Coruña, CTC, CITIC, 15403, Ferrol, A Coruña, Spain.*

JOSÉ-LUIS CASTELEIRO-ROCA**, *Department of Industrial Engineering, University of A Coruña, CTC, CITIC, 15403, Ferrol, A Coruña, Spain.*

HUBERT BERGER†, *FH Joanneum, University of Applied Sciences, 8605, Kapfenberg, Austria.*

DRAGAN SIMIĆ††, *Faculty of Technical Sciences, University of Novi Sad, Trg Dositeja Obradovića 6, 21000, Novi Sad, Serbia.*

JOSÉ-LUIS CALVO-ROLLE§, *Department of Industrial Engineering, University of A Coruña, CTC, CITIC, 15403, Ferrol, A Coruña, Spain.*

Abstract

A dimensional reduction algorithm is applied to an intelligent classification model with the purpose of improving the efficiency and accuracy. The proposed classification model, used to distinguish the operating mode: Hard- and Soft-Switching, is presented and an analysis of the synchronized rectified step-down converter is done. With the aim of improving the accuracy and reducing the computational cost of the model, three different methods for dimensional reduction are applied to the input dataset of the model: self-organizing maps, principal component analysis and correlation matrix. The obtained results show how the number of variable is highly reduced and the performance of the classification model is boosted: the results manifest an improve in the accuracy and efficiency of the classification.

Keywords: Hard-Switching, Soft-Switching, synchronized rectifier, step-down converter, power electronics, classification, dimensional reduction

1 Introduction

The increase of interest in the electric vehicles, Smart Grid and the strong introduction of the renewable energies into the electric systems lead to the rise of research in the field of the

*E-mail: luis.alfonso.fernandez.serantes@udc.es
**E-mail: jose.luis.casteleiro@udc.es
†E-mail: hubert.berger@fh-joanneum.at
††E-mail: dsimic@eunet.rs
§E-mail: jose.rolle@udc.es

Vol. 00, No. 00, © The Author(s) 2024. Published by Oxford University Press.

https://doi.org/10.1093/jigpal/jzae036

power electronics [1, 3, 22]. Nowadays, plenty of companies and universities start focusing in the development of power converters, with incentives such as prices or awards, such as the Little Box Challenge [22].

In the past, most of the research were bringing up new topologies of power converters; however, in the past years, most of the research is focus on the efficiency improve of the existing converters. Consequently, the center of attention is the reduction of weight and size of the power electronic circuits. With the introduction of new semiconductors, such as the Silicon Carbide (SiC) and the Gallium Nitride (GaN) [1, 3], the industry is focusing on their advantages to improve the existing topologies. Some of the remarkable characteristics of these materials in comparison with the traditional silicon are: higher breakdown voltages, lower conduction resistance, higher switching speeds, better thermal dissipation, etc. [1]

In addition to the introduction of new materials, other techniques are also used to reduce the losses. For example, replacing the diodes by transistors lowers the conduction resistance and avoids the on-state voltage drop of the diodes [6]. Furthermore, switching schemes that aim to reduce the losses are highly used, such as the zero current or zero voltage switching. Those techniques achieve Soft-Switching commutation in contrast with the Hard-Switching. In those cases, either the current or the voltage drops to zero before the commutation happens, thus reducing the losses. Some examples of converter topologies, which are based in this operation mode, are the LLC (inductor-inductor-capacitance) resonance converter, operating at the resonance frequency of the components, the Dual-Active-Bridge that operates based on the phase shift between the primary and secondary side of the converter and achieves ZVS or the quasi-resonant flyback converter operation, switching the transistor at a voltage valley [12, 26].

With the introduction of the new materials, the Soft-Switching techniques become more attractive thanks to the improvements in the transistors characteristics [22].

The Artificial Intelligence (AI) is becoming also part of the power electronics field [8, 9, 21]. The AI is expanding in almost all research areas, developing systems that support the engineers in the design and development process of the power converters. There are already some research done in the field of power electronics, such as in [11, 24], where the intelligent techniques are used to design power inductors and transformers, making the design more intuitive and providing accurate results without using complex physic equations and avoiding the iteration between manufacturing samples. Moreover, the researchers also develop control algorithms based on intelligent control such as in [27, 28], where the authors present an intelligent maximum power point tracking control for wind energy conversion systems, tracking the maximum power in real time or a neural-network-based color control method for multi-color LED systems.

The operation mode of the power converter, either Hard- or Soft-Switching, determines the power losses and the efficiency of the converter, therefore its classification becomes very important. If the converter operates in Hard-Switching mode, the switching losses will reduce the efficiency and increase the temperature of the converter thus, increasing the necessary cooling system. On the other hand, if the converter operates in Soft-Switching, the losses can be reduced, thus the temperature and the overall size of the unit.

In this article, a novel method for detecting and classifying the switching mode of the converter is presented. This approach applies the AI in the field of the power electronics. The detection and classification allows the controller to modify the converter parameters, such as the switching frequency or dead-time with the aim of moving the operation mode to SS, increasing in this manner the efficiency of the overall system.

Maintaining the power converter operating in SS mode independently of the load is very important, as the losses increases when the converter is in HS mode. The classifier presented can

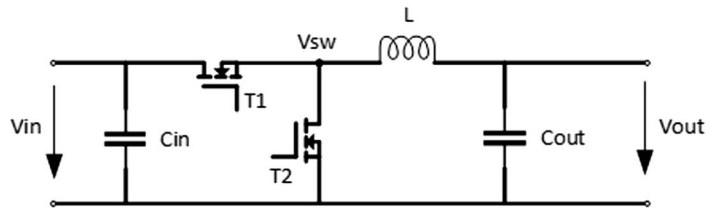

FIGURE 1. Synchronous rectifier step-down converter (half-bridge).

be used for the control of the converter, to maintain its operation point at SS. With the aim of reducing the computational cost of the classifier, so that the intelligent algorithm can be placed in a micro controller, this paper presents different methods to reduce the input variables to the model and reducing in this manner the effort of the model maintaining the accuracy and efficiency of the classifier. The reduced dataset is used as the input of the classification intelligent model.

The document is structured as follows: an analysis of a synchronized rectifier step-down converter is done in the Section 2. Then, the model approach in Section 3 presents the dataset used as well as the structure of the classification model and how the dimensional reduction of the data is applied. Afterwards, in Section 4, the results are presented: the performance of the dimensional reduction methods as well as the accuracy of the classifier are shown and, finally, the conclusions are drawn in Section 5.

2 Case study

In this section, the switching operation modes of the synchronous rectifier step-down converter are explained. This topology has been chosen as it is based on a half-bridge topology, which is used in many other converter topologies, like the synchronous rectifier step-up, the half-bridge LLC, the full-bridge, an inverter... This converter has the following components as shown in Figure 1:

- Switches: there are two switches, the high-side (T1) and the low-side (T2) switch. Their operation is complementary, which means that when one is turn-on, the other will be turn-off. Usually, the switch types used are MOSFETs transistors, as their switching characteristics makes them appropriate to power conversion systems.
- Inductor (L): this part stores the energy when the high-side switch is on and releases the energy when it is off. Additionally, the switching generated pulses are filtered.
- Input capacitor (Cin): it maintains the input voltage constant and provides the peak current, with a low inductive path, to the power switches, reducing the generated noise in the input voltage.
- Output capacitor (Cout): filters the squared pulsed signal generated by the switches while maintaining the output voltage constant.

The Figure 1 shows the circuit scheme of the converter used in this research. The input capacitor is connected to the input voltage and in parallel to the power switches. The middle point between the power switches is called switching node (Vsw in Figure 1) and, after the output filter compound by the inductor and output capacitor, the constant output voltage is generated.

With the aim of explaining the operation principle of the circuit, Figure 2 shows the generated pulsed voltage at the switching node. The sequence is as follows: first, the high-side switch is turned-off and blocking the input voltage. When the gate signal is applied to the high-side transistor, it starts commuting; the current starts rising when the channel starts to build up while the voltage across the device starts dropping until the voltage reaches zero and the full current is driven. During the

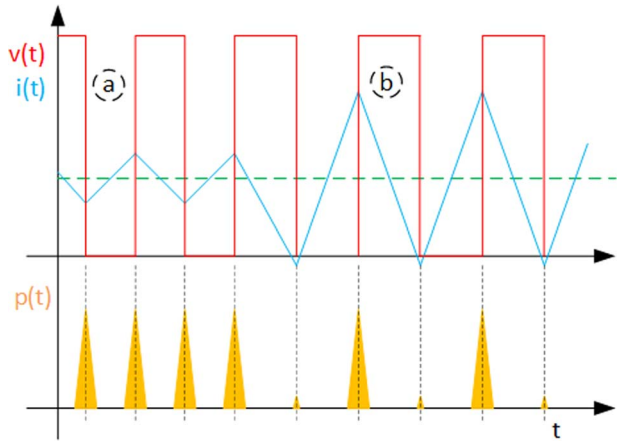

FIGURE 2. Hard- and Soft-Switching transitions with different current ripple.

transition while the current and voltage is present at the transistor's channel, the turn-on switching losses happen.

During the duty cycle, when the high-side transistor keeps conducting and the low-side transistor open, the current starts rising at the inductor.

Then, when the turn-off process starts, the high-side gate signal is set to low, the channel starts closing, so the current flow decreases while the voltage across the device rises. Again, the losses during this transition are called turn-off switching losses.

During this time until the duty cycle starts again, the current at the inductor decreases.

Additional to the explained switching losses, during the conduction of the transistors and due to the on-state resistance, there are conduction losses on the device.

In this case, when during the switching transitions there is voltage and current through the devices, the operating mode is called Hard-Switching (HS) mode.

Moreover, with the aim of avoiding a short circuit during the commutation between the high-side switch drain and low-side switch source, through the transistors, a deadtime is introduced. The deadtime is a time between switching a high-side switch and a low-side switch. During this time that both transistors are off, the current flows through the parasitic diode of the transistors.

The other operating mode of the converter is called Soft-Switching (SS) mode. In this case, either the current or voltage is zero when the switching transition happens. In the case that the current is zero, then the SS mode is Zero Current Switching (ZCS) while if the voltage is zero, then the SS is due to Zero Voltage Switching (ZVS).

In this research, the aim is that the synchronous rectifier step-down converter is only operated in SS, more exactly in ZVS mode. As shown in the Figure 2, part b, the current drops to zero but even goes below zero when the low-side switch is turned-on. At the switching instant, when the current is already negative, the low-side transistor is switched off, so both transistors are off during the deadtime. As the current is flowing towards the switching node, the capacitances of the transistors starts charging and building up voltage. Once this voltage reaches the input voltage, the high-side transistor can switch with zero voltage [20].

In other power converter topologies, such as the full-bridge LLC, the ZCS is achieved by the resonance of components in the circuit that makes the voltage/current to drop; in case of the LLC the resonance tank is between an inductor and a capacitor.

In the design of this converter with the aim of operating in SS mode, the output inductor plays a key role. The inductor needs to be dimensioned in a way that high ripple is allowed. In traditional Hard-Switched step-down converters, the inductor ripple is kept between 10-30% (usually 20%) of the average output current. In this case, the output capacitor effort to filter the output voltage is low, with low current ripple. The selection of the right inductance is done according to the equation 1, as a function of the input voltage, the working cycle, the frequency and the current ripple.

$$L = \frac{(V_{in} - V_{out}) \cdot D}{f \cdot I_{ripple}} \tag{1}$$

where L is the inductance value of the inductor, V_{in} is the input voltage to the circuit, V_{out} is the output voltage from the converter, D is the duty cycle, f is the switching frequency and I_{ripple} is the current ripple in the inductor.

On the other hand, in the case of SS, the current ripple is increased above 200% of the average output current, allowing a swing of current below zero amps, as in [7, 22].

As shown in Figure 2, when the current ripple is kept at around 20% of the average output current, the converter is operated in HS mode, therefore there are switching losses. In contrast, in the b part of the Figure 2, the current ripple is higher than 200%, dropping the current below zero amps, achieving in this way SS.

The main drawbacks of having such a high current ripple is the increase of the Root Means Square (RMS) current and the high ripple in the inductor, which causes high core losses. Moreover, the increase of the RMS current causes also higher on-state losses on the transistors, but its effect can be reduced by increasing the switching frequency.

As comparison between the HS and SS mode, the following calculation has been done, achieving a reduction of $23,32W$ / $13,74mW = 1700$ of the switching losses. As explained previously, in HS mode, the current ripple is kept to 20% of the average output current while in SS, the ripple is 220%. Considering then a switching frequency of 500kHz, a load current of 8A and the used transistor are the GS66516T [10]; the switching losses calculations results in:

Hard-Switching mode:

$$P_{Coss} = \frac{1}{2} C_{oss} \cdot f_{sw} \cdot V^2 = 0.5 \cdot 335pF \cdot 500kHz \cdot 400V^2 = 13,4W \tag{2}$$

$$P_{VI} = \frac{1}{2} V \cdot I_{avg} \cdot t_r \cdot f_{sw} = 0.5 \cdot 400V \cdot 8A \cdot 12,4ns \cdot 500kHz = 9,92W \tag{3}$$

$$P_{sw} = P_{Coss} + P_{VI} = 13,4 + 9,92 = 23,32W \tag{4}$$

Soft-Switching mode:

$$P_{sw} = \frac{1}{2} C_{oss} \cdot f_{sw} \cdot V^2 = 0.5 \cdot 335pF \cdot 500kHz \cdot 4V^2 = 1,34mW \tag{5}$$

$$P_{VI} = \frac{1}{2} V \cdot I_{avg} \cdot t_r \cdot f_{sw} = 0.5 \cdot 4V \cdot (-1A) \cdot 12,4ns \cdot 500kHz = 12,4mW \tag{6}$$

$$P_{sw} = P_{Coss} + P_{VI} = 1,34mW + 12,4mW = 13,74mW \tag{7}$$

3 Model approach

In this article, a classification model with dimensional reduction of its input variables has been implemented. The model is used to classify between the two different operating modes of the

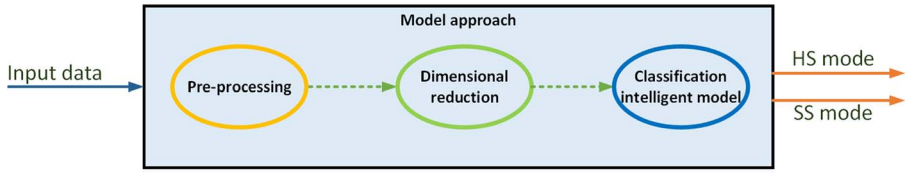

FIGURE 3. Model approach.

synchronous rectifier step-down converter. The dimensional reduction has been done with the aim of reducing the input variables and the computational effort of the classification algorithm.

The Figure 3 shows the procedure from obtaining the simulation data until the output of the classifier is generated. In a first, the data is pre-processed with the aim of obtaining more significant variables. Then, from all the variables, the dimensional reduction is applied and the more representatives are taken to run the classification model. And finally, the classification model provides the operating mode of the power converter.

3.1 Dataset

The synchronous rectifier step-down converter, from the Figure 1, is simulated with the simulation tool LTSpice. Both HS and SS mode are simulated and from the obtained results the dataset is created. Different loads have been applied at a constant input and output voltages. In this case, the simulation model of the GS66516T [10] from GaN Systems has been used.

The simulation has been run 80 times, obtaining the data for each of them, and a combination of HS and SS simulations was done, corresponding 50% of them to each type of operating mode.

The dataset has been obtained by measuring the following variables:

- Input voltage: an input voltage of 400V is applied.
- Output voltage: the converter is operated to provide an output voltage of 200 V. The allowed maximum output ripple is 5 %.
- Switching node voltage (Vsw node Figure 1): the generated squared signal is a result of the switching of the transistors. The voltage at this node varies from 0 up to 400 V. The switching frequency is variable depending on the simulation case, as it is varied to maintain either HS or SS mode. The variation is from 80 kHz to 2 MHz.
- Inductor current: varies according to a triangular shape. When the input voltage is applied, the current rises while it decreases when the low-side switch is on. When the converter operates in HS, the ripple of the current is 20 % of the output average current while in SS, the current ripple is 220%, ensuring that the current drops below zero amps.
- Output current: value that depends on the applied load.

Then, the imported data is analysed and processed to obtain more representative variables for the classification mode. From the raw data, the most representative signal is the switching node voltage, as it reflects how the transition occurs. Therefore, from the switching node signal the following variables are obtained:

The first and second derivative are derived from the signal. It provides information of the changes in the switching voltage and how fast those changes are. Moreover, it removes the on- and off-states of the signal as the first derivative is equal to zero.

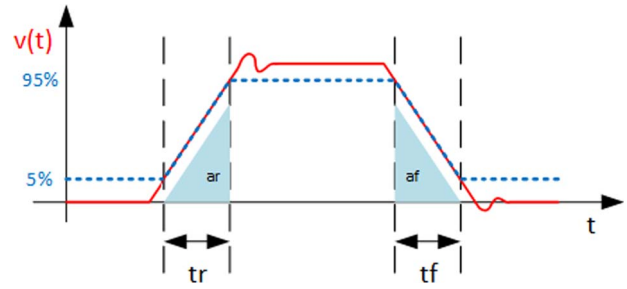

FIGURE 4. Rising and falling edge of the switching node voltage, in dashed blue, and the original signal in continuous red.

The rising and falling transitions are also separated. The Figure 4 shows how the separation is done. Once the switching node voltage reaches 5%, the data is stored until the voltage reaches 95% of the input voltage. This new signal provides information about the rising and falling timing (*tr* and *tf* , respectively). Moreover, the first and second derivatives are also applied to the obtained data from the rising and falling transitions and, the integral of this signal is also calculated, providing the area under the signal (*ar* and *af*), as shown in the Figure 4.

As described above, 8 new signals has been derived from the switching node voltage: the raw data (red signal in Figure 4), the first and the second derivatives of the raw data, the rising/falling edge data (dotted blue signal in Figure 4), the first and second derivatives of rising/falling edge data, the rising edge integral (area at the rising edge, *ar*, in Figure 4) and the falling edge integral (area at the falling edge, *af* , in Figure 4).

With the aim of simplifying further the data and obtaining more significant dataset, the following statistics have been calculated for each of the 8 variables: average, standard deviation, variance, co-variance, RMS and Total Harmonic Distortion (THD). Resulting in a matrix of 8x6 for each of the 80 simulations.

3.2 Methods

In this research three dimensional reduction algorithms have been used: SOM (Self-Organizing Map), PCA (Principal Component Analysis) and the correlation matrix.

3.2.1 Self-Organizing Map (SOM) This algorithm can be used to create clusters data and also to reduce the dimensionality of the data. The technique assigns data to clusters based on similarity and topology trying to assign the same number of instance to each group [5].

3.2.2 Principal Component Analysis (PCA) One of the classical algorithm used to dimensional reduction is the PCA. This technique guarantees the minimum MSE and gain linearly independent vectors as the basis of subspace [15, 17].

3.2.3 Correlation matrix The correlation matrix is a table that shows the relations coefficients between variables; each cell correspond to the correlation between two variables. This technique summarize data, and it is used as preliminary analysis before apply advanced algorithms, and also to diagnosis the advanced analysis [15, 17].

3.3 Classification model

3.3.1 Multilayer perceptron A typical organization of several neurons is the multilayer perceptron. The internal structure divides the neurons in one input layer, one output layer and several hidden (or internal) layers. All the layers are connected between the previous and the follows one, all but input and output ones, that are connected to the inputs and outputs of the model [13, 23].

3.3.2 Linear discriminant analysis This method projects the data from a high dimensional space into a low-dimensional space. This method uses a weight vector W, which projects the given set of data vector E in such a way that maximizes the class separation of the data but minimizes the intra-class data [4]. The separation is good when the projections of the class involves exposing long distance along the direction of vector W [19].

$$P_i = W^T E_i \tag{8}$$

The LDA provides each sample with its projection and the class label. Two outputs are provided by the analysis, first a gradual decision that is then converted into a binary decision. This method maximizes ratio between the inter-class variance to the intra-class variance, finding the best separation of the classes. The performance of the method increases with the distance between the samples [16, 19].

3.3.3 Support vector machine This algorithm perform a data projection throw a kernel operator that allows to increase the dimensional feature of the data. In the new feature space, the algorithm try to maximize the minimum distance between two parallel hyperplanes that define the class of samples [18].

3.3.4 Ensemble The term ensemble is used to define multiple classification methods that are used in combination with the aim of improving the performance over single classifiers [25]. They are commonly used for classification tasks. The ensemble does a regularization, process of choosing fewer weak learners in order to increase predictive performance [14].

3.3.5 Confusion matrix To validate the models, the predicted outputs are compared with data that has been correctly classified and this comparison is summarize in a confusion matrix. The confusion matrix assesses the quality of a classifier. The entry to this matrix are the true values and the predicted values, where the true values compound the columns while the predicted ones the rows [2].

SEnsitivity (SE), SPeCificity (SPC), Positive Prediction Value (PPV), Negative Prediction Value (NPV) and Accuracy (ACC) are the five statistics indicators used to analysed the performance of the models [2].

3.4 Experiments description

The initial dataset is used to train the different models and, then, validate the improvement of the performance by the dimensional reduction.

The data is divided into two sub-sets, one used to train the different models, 75 % of the data, and other set used to validate the model, the rest 25 %. The division of the dataset is done randomly.

Once the data is grouped in two sets, the different models are trained:

- MLP: the chosen algorithm is the Levenberg–Marquardt backpropagation and trained from 1 to 10 neurons on the hidden layers.

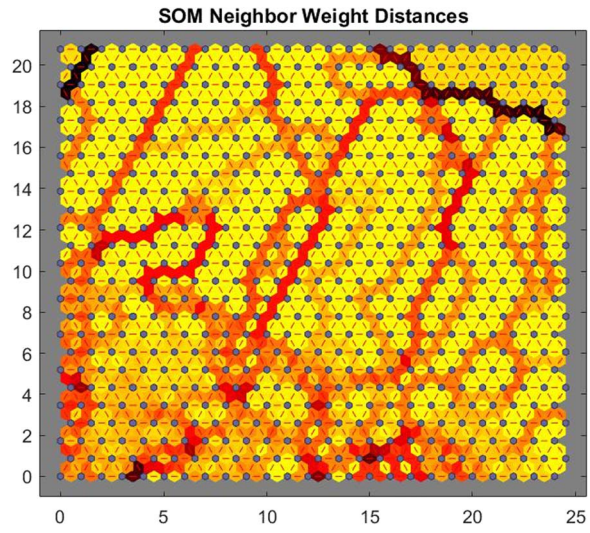

FIGURE 5. Model approach.

- LDA: the discriminant type is the regularized LDA.
- SVM: The SVM has been trained using the linear kernel function.
- Ensemble: the used method is an adaptive logistic regression with number of cycles from 10 to 100 in steps of 10.

Then, the validation data is used to check if the models have been correctly trained. The predictions obtained from the models are compared with the verified data, using a confusion matrix and the different statistics are calculated.

In other step, the data is normalized with the aim of unifying the different measurements. This dataset is then used as input to the model, so that we can compare the performance as well by just using normalized data.

Furthermore, we apply the the following methods to reduce the variables and dimensions of the model, improving in this way the performance and reducing the computational cost of the model:

- SOM: Train with size of 20 two-dimensional map. The different maps for each variable are compared, removing the similar maps and keeping the most relevant variables.
- Correlation matrix: the values close to 1 or -1 indicate that there is a linear relationship between the data columns and they can be removed, leaving the values that are equal or close to 0, that suggest that these data are not related. The chosen limit to differentiate the variables is 0.33.
- PCA: creates a new matrix that keeps the most relevant features of the input data, removing the redundant information.

4 Results

First of all, the obtained results of the model without using any of the presented dimensional reduction methods are shown in the Table 1. The best result obtained without dimensional reduction is achieved by the MLP7 with an accuracy of 0.97059.

TABLE 1. Results without dimensional reduction methods.

	Sensitivity	Specificity	Negative prediction value	Positive prediction value	Accuracy
MLP1	0.72727	1	0.63636	1	0.81538
MLP2	0.65385	1	0.47059	1	0.73529
MLP3	0.63462	0	0	0.97059	0.62264
MLP4	0.53125	1	0.11765	1	0.55882
MLP5	0.70833	1	0.58824	1	0.79412
MLP6	0.55738	1	0.20588	1	0.60294
MLP7	0.94444	1	0.94118	1	0.97059
MLP8	0.65385	1	0.47059	1	0.73529
MLP9	0.7907	1	0.73529	1	0.86765
MLP10	0.51515	1	0.058824	1	0.52941
SVM	0.69388	1	0.55882	1	0.77941
LDA	0.55738	1	0.20588	1	0.60294
En. 10-100	0.50746	1	0.029412	1	0.51471

TABLE 2. SOM groups.

	1				8										
	5		6		11		12								
	31	2-4	36		14	9-10	18			24					
Groups	35	32-34	42	7	17	15-16	48	13	19-23	30	25-29	37	38-41	43	44-47
Taken variable	1	2	6	7	8	9	12	13	19	24	9	37	38	43	44

TABLE 3. Summary of the results from SOM.

	Sensitivity	Specificity	Negative prediction value	Positive prediction value	Accuracy
MLP1	0.83333	0.95	0.86364	0.9375	0.89474
MLP2	0.88889	1	0.90909	1	0.94737
MLP3	0.88889	1	0.90909	1	0.94737
MLP4	1	1	1	1	1
MLP5	0.82353	0.89474	0.85	0.875	0.86111
MLP6	0.84211	1	0.86364	1	0.92105
MLP7	1	1	1	1	1
MLP8	0.84211	1	0.86364	1	0.92105
MLP9	1	0.95652	1	0.9375	0.97368
MLP10	1	1	1	1	1
SVM	0.88889	1	0.90909	1	0.94737
LDA	0.7619	1	0.77273	1	0.86842
En. 10	0.94118	1	0.95455	1	0.97368
En. 20-100	0.88889	1	0.90909	1	0.94737

When SOM is used, due to similarity of the data, 33 variables are removed from the dataset, reducing the size in a almost 70 %.

TABLE 4. Groups of the correlation matrix.

Groups											
	1 5 31 35	2-4 6 8 11 19-24	7-12	13-17	25-29	30 32-34	36 38-40	37-41	42	43	44-48
Taken variable	1	2	7	13	25	30	36	37	42	43	44

TABLE 5. Summary of the results from the correlation matrix.

	Sensitivity	Specificity	Negative prediction value	Positive prediction value	Accuracy
MLP1	0.88235	0.95	0.90476	0.9375	0.91892
MLP2	0.88889	1	0.90476	1	0.94595
MLP3	0.88889	1	0.90476	1	0.94595
MLP4	1	1	1	1	1
MLP5	0.88889	1	0.90476	1	0.94595
MLP6	0.84211	1	0.86364	1	0.92105
MLP7	0.94118	1	0.95238	1	0.97297
MLP8	0.88889	1	0.90476	1	0.94595
MLP9	1	1	1	1	1
MLP10	0.94118	1	0.95238	1	0.97297
SVM	0.88235	0.95	0.90476	0.9375	0.91892
LDA	0.9375	0.95238	0.95238	0.9375	0.94595
En. 10	0.8	1	0.80952	1	0.89189
En. 20	0.78947	0.94444	0.80952	0.9375	0.86486

The reduction of the groups done with the SOM method are shown in the Table 2, while the obtained results of the classification model when the SOM dataset is used are shown in the Table 3. When SOM is used, the performance of the model increases, taking special attention to the accuracy increase of the ensemble model.

In the correlation matrix, 37 variables are removed from the dataset, reducing the size in a almost 78 %. The groups of data done with the correlation matrix are shown in the Table 4. In this case, the performance of the model is also increased, and also showing better accuracy with the ensemble technique. The Table 5 shows the results.

On the other hand, when the PCA dimensional reduction method is used, the performance and accuracy of the classification models are reduced, but with a slightly increase of the ensemble accuracy. The Table 6 shows the results obtained with the PCA method.

Finally, as a summary of all the classification models with the different dimensional reduction techniques, the Table 7 shows the obtained performance.

TABLE 6. Summary of the results from PCA.

	Sensitivity	Specificity	Negative prediction value	Positive prediction value	Accuracy
MLP1	0.33333	0	0	0.66667	0.28571
MLP2	0.36364	NaN	0	1	0.36364
MLP3	0.25	0.33333	0.18182	0.42857	0.27778
MLP4	0.4	0.44444	0.4	0.44444	0.42105
MLP5	0.2	0.5	0.38462	0.28571	0.35
MLP6	0.54545	0.5	0.375	0.66667	0.52941
MLP7	0.23077	0.25	0.090909	0.5	0.23529
MLP8	0.3	0.55556	0.41667	0.42857	0.42105
MLP9	0.3	0.5	0.36364	0.42857	0.38889
MLP10	0.15385	0.3	0.21429	0.22222	0.21739
SVM	0.33333	0.46154	0.375	0.41667	0.39286
LDA	0.38462	0.53333	0.5	0.41667	0.46429
En. 10-100	0.92308	1	0.9375	1	0.96429

TABLE 7. Summary of the results.

Classification method	Dimensional reduction methods			
	Without reduction	SOM	Corr. Matrix	PCA
MLP1	0.81538	0.89474	0.91892	0.28571
MLP2	0.73529	0.94737	0.94595	0.36364
MLP3	0.62264	0.94737	0.94595	0.27778
MLP4	0.55882	1	1	0.42105
MLP5	0.79412	0.86111	0.94595	0.35
MLP6	0.60294	0.92105	0.92105	0.52941
MLP7	0.97059	1	0.97297	0.23529
MLP8	0.73529	0.92105	0.94595	0.42105
MLP9	0.86765	0.97368	1	0.38889
MLP10	0.52941	1	0.97297	0.21739
SVM	0.77941	0.94737	0.91892	0.39286
LDA	0.60294	0.86842	0.94595	0.46429
En. 10	0.51471	0.97368	0.89189	0.96429
En. 20-100	0.51471	0.94737	0.86486	0.96429

5 Conclusions and future works

In this paper the dimensional reduction of the input dataset used by classification model has been implemented. The classifier distinguish between the operating modes of a step-down converter.

Three different dimensional reduction methods have been applied to the input dataset of the classifier. The self-organized map creates clusters based on similarity and the most relevant clusters are kept, the correlation matrix provides the relation coefficients between the variables, allowing

to reduce the input variables that are related while the principal component analysis creates a new matrix that keeps the most relevant features of the input data, removing the redundant information.

The different proposed methods achieved different reduction rates: while SOM achieve 70% of data reduction, the correlation matrix achieve 78%.

Additionally, the performance and accuracy of the classification model have been increased by the dimensional reduction of the dataset. Thus, a 100% of classification accuracy for the MLP4, MLP5 and MLP10 is achieved when the SOM technique was used. Furthermore, when the correlation matrix was used, the performance of the classification method reaches the 100% with the MLP4 and MLP9.

On the other hand, the PCA technique does not achieve a classification of 100% with any model but improves the performance of the Ensemble models.

In conclusion, the proposed dimensional reduction has improved the performance of the classification model as well as reducing the computational efforts, improving the overall efficiency. In this manner, the proposed intelligent system supports the design process of the converters and increases the energy efficiency.

With the aim of continuing this research, a hybrid intelligent model will be implemented, for the purpose of improving the classification accuracy up to 100%. In a further step, the model will be implemented in the control loop of the power converter, detecting, classifying the operating mode and reacting on it to achieve SS mode all over the operating range.

Funding

Funding for open access charge: Universidade da Coruña/CISUG.

References

[1] A. M. S. Al-bayati, S. S. Alharbi, S. S. Alharbi and M. Matin. A comparative design and performance study of a non-isolated dc-dc buck converter based on si-mosfet/si-diode, sic-jfet/sic-schottky diode, and Gan-transistor/sic-schottky diode power devices. In *2017 North American Power Symposium (NAPS)*, pp. 1–6, 2017.

[2] J. L. Calvo-Rolle and E. Corchado. A bio-inspired knowledge system for improving combined cycle plant control tuning. *Neurocomputing*, **126**, 95–105, 2014.

[3] J.-L. Casteleiro-Roca, A. J. Barragan, F. Segura, J. L. Calvo-Rolle and J. M. Andujar. Intelligent hybrid system for the prediction of the voltage-current characteristic curve of a hydrogen-based fuel cell. *Revista Iberoamericana de Automática e Informática Industrial*, **16**, 492–501, 2019.

[4] J.-L. Casteleiro-Roca, A. J. Barragan, F. Segura, J. L. Calvo-Rolle and J. M. Andujar. Intelligent hybrid system for the prediction of the voltage-current characteristic curve of a hydrogen-based fuel cell. *Revista Iberoamericana de Automática e Informática Industrial*, **16**, 492–501, 2019.

[5] C. Crespo-Turrado, J. L. Casteleiro-Roca, F. Sánchez-Lasheras, J. A. López-Vázquez, F. J. D. C. Juez, F. J. P. Castelo, J. L. Calvo-Rolle and E. Corchado. Comparative study of imputation algorithms applied to the prediction of student performance. *Logic Journal of the IGPL*, **28**, 58–70, 2020.

[6] H. Eraydin and A. F. Bakan. Efficiency comparison of asynchronous and synchronous buck converter. In *2020 6th International Conference on Electric Power and Energy Conversion Systems (EPECS)*, pp. 30–33, 2020.

[7] L. A. Fernandez-Serantes, H. Berger, W. Stocksreiter and G. Weis. Ultra-high frequent switching with Gan-hemts using the coss-capacitances as non-dissipative snubbers. In *PCIM*

Europe 2016; International Exhibition and Conference for Power Electronics, Intelligent Motion, Renewable Energy and Energy Management, pp. 1–8. VDE, 2016.

[8] L. A. Fernandez-Serantes, J. L. Casteleiro-Roca and J. L. Calvo-Rolle. Sistema híbrido inteligente para el control y operación de un convertidor elevador en modo soft-switching. *Revista Iberoamericana de Automática e Informática industrial*, **19**, 356–368, 2022.

[9] L. A. Fernández-Serantes, R. E. Vázquez, J. L. Casteleiro-Roca, J. L. Calvo-Rolle and E. Corchado. Hybrid intelligent model to predict the soc of a lfp power cell type. In *International Conference on Hybrid Artificial Intelligence Systems*, pp. 561–572. Springer, 2014.

[10] GaN Systems Inc. *GS66516T Top-Side Cooled 650 V E-Mode GaN Transistor*, 2018. Rev 180422.

[11] T. Guillod, P. Papamanolis and J. W. Kolar. Artificial neural network (ann) based fast and accurate inductor modeling and design. *IEEE Open Journal of Power Electronics*, **1**, 284–299, 2020.

[12] G.-C. Huang, T.-J. Liang and K.-H. Chen. Losses analysis and low standby losses quasi-resonant flyback converter design. In *2012 IEEE International Symposium on Circuits and Systems (ISCAS)*, pp. 217–220, 2012.

[13] E. Jove, J. Casteleiro-Roca, H. Quintián, J. A. Méndez-Pérez and J. L. Calvo-Rolle. Anomaly detection based on intelligent techniques over a bicomponent production plant used on wind generator blades manufacturing. *Revista Iberoamericana de Automática e Informática Industrial*, **17**, 84–93, 2020.

[14] E. Jove, J. Casteleiro-Roca, H. Quintián, J. A. Méndez-Pérez and J. L. Calvo-Rolle. Anomaly detection based on intelligent techniques over a bicomponent production plant used on wind generator blades manufacturing. *Revista Iberoamericana de Automática e Informática Industrial*, **17**, 84–93, 2020.

[15] E. Jove, P. Blanco-Rodríguez, J.-L. Casteleiro-Roca, H. Quintián, F. J. M. Arboleda, J. A. LóPez-Vázquez, B. A. Rodríguez-Gómez, M. Del Carmen, A. P.-P. Meizoso-López and F. J. D. C. Juez. Missing data imputation over academic records of electrical engineering students. *Logic Journal of the IGPL*, **28**, 487–501, 2020.

[16] E. Jove, P. Blanco-Rodríguez, J.-L. Casteleiro-Roca, H. Quintián, F. J. M. Arboleda, J. A. LóPez-Vázquez, B. A. Rodríguez-Gómez, M. Del Carmen, A. P.-P. Meizoso-López and F. J. D. C. Juez., et al. Missing data imputation over academic records of electrical engineering students. *Logic Journal of the IGPL*, **28**, 487–501, 2020.

[17] E. Jove, J.-L. Casteleiro-Roca, H. Quintián, D. Simić, J.-A. Méndez-Pérez and J. L. Calvo-Rolle. Anomaly detection based on one-class intelligent techniques over a control level plant. *Logic Journal of the IGPL*, **28**, 502–518, 2020.

[18] E. Jove, J. M. Gonzalez-Cava, J.-L. Casteleiro-Roca, J.-A. Méndez-Pérez, J. A. Reboso-Morales, F. J. Pérez-Castelo, F. Javier and M. de Cos Juez, and José Luis Calvo-Rolle. Modelling the hypnotic patient response in general anaesthesia using intelligent models. *Logic Journal of the IGPL*, **27**, 189–201, 2019.

[19] J. L. Casteleiro-Roca, H. Quintián, J. L. Calvo-Rolle, J.-A. Méndez-Pérez, F. J. Perez-Castelo and E. Corchado. Lithium iron phosphate power cell fault detection system based on hybrid intelligent system. *Logic Journal of the IGPL*, **28**, 71–82, 2020.

[20] N. Mohan, T. M. Undeland and W. P. Robbins. *Power Electronics: Converters, Applications, and Design*. John Wiley & Sons, 2003.

[21] J.-A. Montero-Sousa, L.-A. Fernandez-Serantes, J.-L. Casteleiro-Roca, X.-M. Vilar-Martnez

and J.-L. Calvo-Rolle. *Energy Storage Management for Generation-Distribution Facilities*, 2017.

[22] D. Neumayr, D. Bortis and J. W. Kolar. The essence of the little box challenge-part a: key design challenges solutions. *CPSS Transactions on Power Electronics and Applications*, **5**, 158–179, 2020.

[23] S. Tahiliani, S. Sreeni and C. B. Moorthy. A multilayer perceptron approach to track maximum power in wind power generation systems. In *TENCON 2019—2019 IEEE Region 10 Conference (TENCON)*, pp. 587–591, 2019.

[24] T. Liu, W. Zhang and Z. Yu. Modeling of spiral inductors using artificial neural network. In *Proceedings. 2005 IEEE International Joint Conference on Neural Networks, 2005*, vol. 4, pp. 2353–2358, 2005.

[25] R. V. Vega, H. Quintián, J. L. Calvo-Rolle, Á. Herrero and E. Corchado. Gaining deep knowledge of android malware families through dimensionality reduction techniques. *Logic Journal of the IGPL*, **27**, 160–176, 2019.

[26] Z. Wang, Z. Lou and H. Chen. A novel dual-llc resonant soft switching converter for super high frequency induction heating power supplies. In *2007 IEEE Power Electronics Specialists Conference*, pp. 2561–2566, 2007.

[27] C. Wei, Z. Zhang, W. Qiao and Q. Liyan. Reinforcement-learning-based intelligent maximum power point tracking control for wind energy conversion systems. *IEEE Transactions on Industrial Electronics*, **62**, 6360–6370, 2015.

[28] X. Zhan, W. Wang and H. Chung. A neural-network-based color control method for multi-color led systems. *IEEE Transactions on Power Electronics*, **34**, 7900–7913, 2018.

Received 20 May 2022